Estuaries and Coasts (2025) 48:12
https://doi.org/10.1007/s12237-024-01455-3

# Satellite-Derived Dissolved Organic Carbon Distribution and Variability in an Interconnected Estuary off the Southeastern U.S

**Renato M. Castelao**[1] · **Patricia M. Medeiros**[1]

Received: 18 May 2024 / Revised: 15 October 2024 / Accepted: 31 October 2024


## Abstract

The Altamaha River estuary off the southeastern U.S. is an important source of dissolved organic carbon (DOC) to the coastal ocean. The estuary is formed by three interconnected sounds, and it is characterized by a complex network of narrow channels and creeks with high spatial heterogeneity, making it difficult to study with in situ observations alone. Here, use used satellite data from Landsat available in high resolution (30 m) to investigate DOC distribution and variability in the system. Our analyses show that DOC variability in the estuary is characterized by two seasonal peaks, one in spring and one in fall, while over the shelf maximum DOC content is observed during summer. A multiple regression analysis was used to quantify physical mechanisms controlling DOC variability in the estuary. In addition to seasonal variations, anomalies in river discharge are the dominant factor controlling DOC variability throughout much of the estuarine system. Tides play a key role near the mouth of each sound and in some upstream regions, likely associated with inputs from salt marshes. The influence of winds is smaller and is restricted to the area near the mouth of the Altamaha Sound. Landsat data also captured an input of ~ 2 Gg of DOC to the estuary associated with the passage of Hurricane Irma in 2017. Our results demonstrate that Landsat can provide useful information about scales of variability in narrow estuaries, including capturing the occurrence of sharp fronts that would be difficult to observe with traditional in situ measurements alone.

**Keywords** Estuarine variability · Dissolved organic carbon · Ocean color · Altamaha River estuary · Landsat · Fronts

## Introduction

Estuaries are important transition zones linking terrestrial and marine ecosystems. Off the southeastern U.S., coastal wetlands are common, playing an important ecological role and affecting carbon sequestration and storage, biological production, and offering flooding and shoreline protection (Odum 1980; Kirwan and Megonigal 2013; Spivak et al. 2019; Ward et al. 2020). Estuaries are highly dynamic systems characterized by strong variability and by complex circulation influenced by tidal currents, river discharge, wind forcing, and steep density gradients (MacCready and Geyer 2010). As a result, variability in estuaries occurs on a continuum of scales (Wolfe and Kjerfve 1986).

Estuaries are also known to play an important role in carbon cycling (Canuel et al. 2012; Bauer et al. 2013; Noriega and Araujo 2014; Canuel and Hardison, 2016; Letourneau et al. 2021; Martineac et al. 2021). Dissolved organic carbon (DOC) concentrations in estuaries are influenced by a variety of processes, including variability in river discharge, marsh-derived inputs, biological production and consumption, photo-chemical degradation and flocculation, in addition to physical processes such as advection and mixing (Hedges et al. 1997; Tzortziou et al. 2008; Osburn et al. 2015, 2019; Moran et al. 2016; among many others). The flux of DOC to estuaries is also often influenced by extreme events (Yoon and Raymond 2012; Miller et al. 2016; Raymond et al. 2016; Letourneau et al. 2021; Medeiros 2022). These processes act on different spatial and temporal scales, and as such DOC concentrations in estuaries are often characterized by high spatial and temporal variability (e.g., Cao and Tzortziou 2021). This makes investigating the distribution and variability of DOC (and of other quantities) in estuaries challenging.

Communicated by Faming Wang

✉ Renato M. Castelao
castelao@uga.edu

[1] Department of Marine Sciences, University of Georgia, Athens, GA, USA

Published online: 07 November 2024

In the southeastern U.S., the Altamaha River estuary is the focus of the Georgia Coastal Ecosystem Long Term Ecological Research (GCE-LTER) program (Alber et al. 2013). The system is formed by three interconnected sounds (Altamaha, Doboy, and Sapelo Sounds; Fig. 1), with freshwater being delivered primarily by the Altamaha River. River discharge is the main control of variability in salinity in the estuary, which varies from 0 in the Altamaha River at the head of the Altamaha Sound to about 32–34 in the coastal ocean (Wang et al. 2017). Tides are semidiurnal, and range in height from 1.8 to 2.4 m during neap to spring tides (Di Iorio and Castelao 2013), and account for most of the cross-shelf current variance (Tebeau and Lee 1979; Lee and Brooks 1979) contributing to estuary-shelf exchange. The estuary is also characterized by high interconnectivity (Wang et al. 2017), with the complex network of creeks and channels playing an important role in water exchange between the three sounds (Di Iorio and Castelao 2013). Previous studies have shown that DOC concentration in the estuary varies substantially among the different sounds (Letourneau et al. 2021), being influenced by variability in river discharge (Letourneau and Medeiros 2019), tides (Martineac et al. 2021), and extreme events such as the passage of tropical storms and hurricanes (Medeiros 2022).

Although many previous studies have investigated variability (Fournier et al. 2015; da Silva and Castelao 2018) and DOC dynamics (Mannino et al. 2008, 2016; Fichot et al. 2014; Liu et al. 2014; Matsuoka et al. 2017; Cao et al. 2018; Martineac et al. 2024) in the coastal ocean and wide estuaries using satellite-derived ocean color data, that remains challenging in estuaries characterized by narrow channels because the resolution of many satellite products is not high enough to resolve those systems. Recently, however, Cao and Tzortziou (2021) developed an algorithm based on Landsat data relating DOC concentration to the spectral shape of water remote sensing reflectance, which allowed them to investigate DOC dynamics in a tidally influenced wetland-estuarine system in Chesapeake Bay, U.S. Because of its high resolution (~ 30 m), Landsat data may be especially suited for investigations in narrow estuaries with complex coastlines and small spatial scales of variability, making them difficult to measure in high resolution with in situ observations alone. Landsat data are now available for over a decade, also allowing for investigations of temporal variability in those systems.

Here, we implemented the algorithm developed by Cao and Tzortziou (2021) for Landsat observations, calibrating it using in situ observations from the Altamaha River estuary. We then used it to investigate DOC distribution in the estuary, as well as to quantify physical controls of DOC variability in the system. Because salinity and DOC concentration in the estuary are correlated to each other (Letourneau et al. 2021; Medeiros 2022), ocean color observations can also provide useful information about variability in the distribution of river-influenced waters in the system (as in Fournier et al. 2015; da Silva and Castelao 2018). Lastly, we also quantified the input of DOC to the estuary associated with the passage of Hurricane Irma in the fall of 2017.

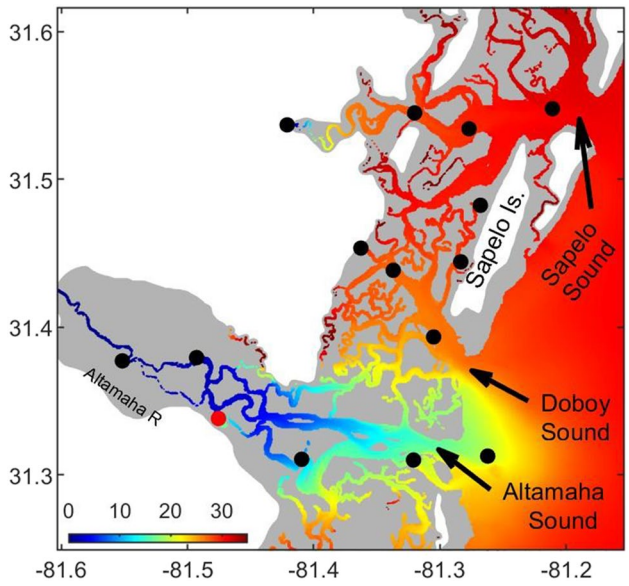


**Fig. 1** Altamaha River estuary off the southeastern U.S. Colors show annual mean salinity from an ocean model (Wang et al. 2017). Circles show locations of in situ DOC measurements (Letourneau et al. 2021) used to calibrate the satellite algorithm. Additional independent DOC observations (Medeiros 2022) are available at the station denoted by a red circle. Uplands and salt marshes are shown in white and gray, respectively

## Methods

### In Situ Observations

In situ observations of DOC concentrations were obtained at 15 stations spanning the Altamaha River estuary (Fig. 1). Observations were collected in April, July, and October 2017 and in January 2018. Sampling procedures and analytical methods used are described in detail in Letourneau et al. (2021). The in situ DOC concentrations were used to calibrate an algorithm to estimate DOC from satellite observations. Additional in situ DOC concentration measurements spanning a few years are available at a station in the Altamaha River (red circle in Fig. 1; Medeiros 2022). We used those observations to independently compare the seasonal evolution of DOC concentrations based on in situ data and satellite measurements.

## Satellite Measurements of DOC Concentrations

We followed the method outlined by Cao and Tzortziou (2021) to obtain satellite-derived estimates of DOC in the Altamaha River estuary. Satellite observations from the Landsat 8 and 9 OLI sensors were obtained from the United States Geological Survey (USGS) Earth Explorer website (https://earthexplorer.usgs.gov). Landsat 8 was launched in 2013, while Landsat 9 was launched in 2021. The revisit time of each of the satellites is approximately 16 days, and the spatial resolution is 30 m. The open-source ACOLITE processor was used to process Level 1 data and generate ocean color remote sensing reflectance (Rrs) measurements at multiple bands. A total of 170 clear-sky images were obtained from 2013 to 2023. Highest data availability generally occurs during fall and winter peaking in January, and minimum availability occurs in May and June (Fig. 2) due to variability in cloud coverage and sun glint contamination.

Satellite observations of Rrs were compared to in situ measurements of DOC to quantify the relationship between those variables. Time intervals between in situ sampling and the collection of the satellite images used for algorithm calibration ranged between 1 and 6 days. Tidal variability is known to influence DOC concentrations and DOM composition in estuaries (e.g., Tzortziou et al. 2008), so ideally in situ and satellite data matchups should include only data from a similar tidal phase (Cao and Tzortziou 2021). Letourneau et al.'s (2021) spatially resolving sampling occurred during 4 quasi-synoptic field efforts during high

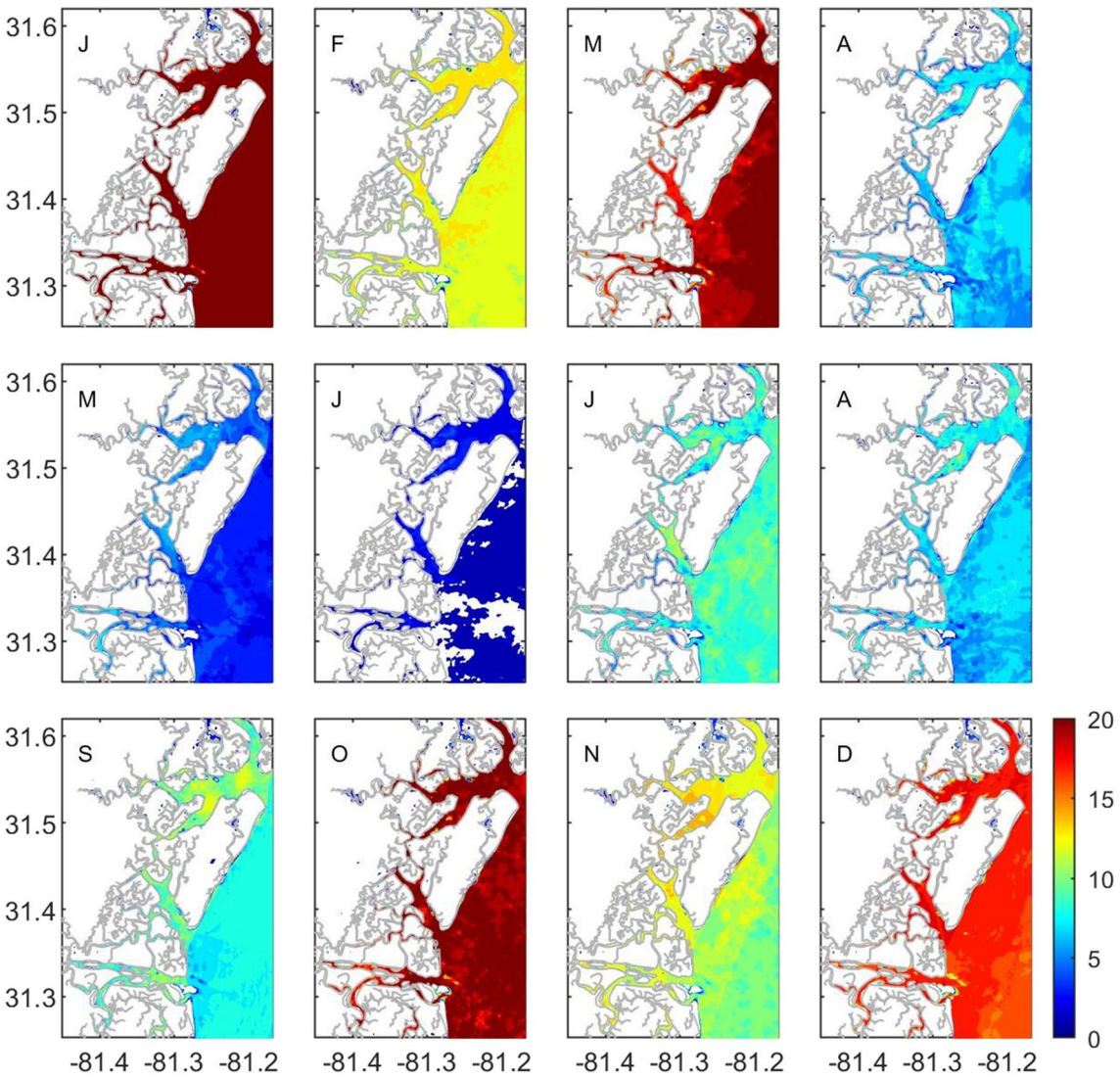


**Fig. 2** Number of available observations from Landsat at the Altamaha River estuary for each month from 2013 to 2023. Availability of observations is influenced by cloud cover and/or sun glint contamination. Number of available observations exceeding 20 are shown in dark red to reveal as much of the spatial pattern as possible

tide, however, and thus did not resolve tidal variability. The implications of using matchups including data from different tidal phases are addressed in the discussion section. A nonlinear regression of the form (Cao and Tzortziou 2021)

$$\mathrm{DOC} = \exp(\alpha + \beta \times \log(\mathrm{Rrs(B1)}) + \gamma \times \log(\mathrm{Rrs(B2)}) + \delta \times \log(\mathrm{Rrs(B3)}) + \xi \times \log(\mathrm{Rrs(B4)})) \quad (1)$$

was used to parameterize the relationship between the satellite measurements of Rrs and the in situ DOC concentration (in µmol $L^{-1}$). In Eq. 1,

$\alpha = 1.752,\ \beta = -0.610,\ \gamma = -1.000,\ \delta = 0.133,$ and $\xi = 0.666$

are the coefficients of the nonlinear regression and B1 to B4 are the spectral bands centered at 443/483/561/655 or 443/482/561/654 nm for Landsat 8 and Landsat 9, respectively. Satellite-derived and in situ point measurements of DOC were found to be significantly correlated (Fig. 3; $r = 0.87$, $p < 0.001$), with root-mean-square error = 46.6 µmol $L^{-1}$ and a mean average percent difference of 11.5 ± 9.8%.

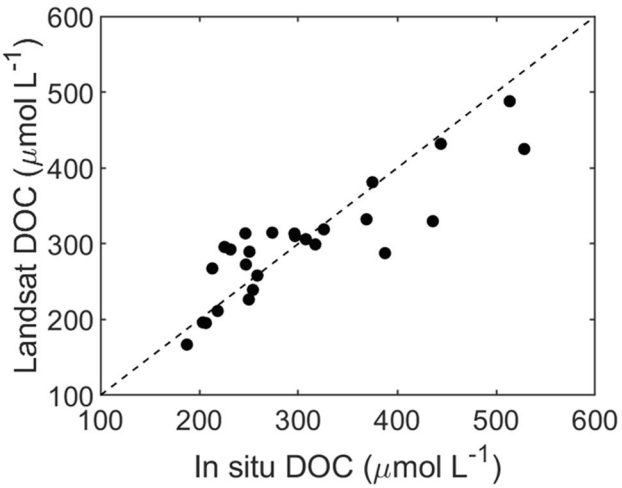


**Fig. 3** Pairing of in situ point measurements of DOC concentration (µmol $L^{-1}$) in the Altamaha River estuary (Letourneau et al. 2021) with satellite-derived DOC concentrations from Landsat calculated using Eq. (1). Dashed line is the 1:1 line

These are comparable to the statistics reported by Cao and Tzortziou (2021) for their algorithm implementation to Chesapeake Bay.

We further evaluated the algorithm by comparing the seasonal evolution of DOC concentrations from Landsat (using Eq. 1) with independent in situ observations collected at the Altamaha River (Medeiros 2022), upstream of the estuarine region (zero salinity; red circle in Fig. 1). In situ observations are primarily from 2015 to 2016, with a few observations from 2017 and 2018. We also estimated the seasonal cycle using two harmonics for both datasets (Fig. 4). Satellite and in situ observations present similar seasonal evolution, with a peak in spring, a local minimum during summer, and a second increase during fall. Although the seasonal evolution is nicely captured by satellite observations, concentrations are generally smaller compared to in situ data. We note that DOC concentrations at this site are generally quite high, often exceeding the range of DOC variability available for developing the algorithm (Fig. 3). Lastly, we also note that although the water depth in the main channels of the estuary can exceed 10 m, smaller channels and creeks are shallower than that. As such, it is possible that the satellite data may be affected by bottom reflectance contamination (e.g., Reichstetter et al. 2015).

## Additional Observations

Sea surface elevation was obtained from tide gauge data downloaded from the University of Hawaii Sea Level Center (https://uhslc.soest.hawaii.edu/network) at Fork Pulaski, GA. Winds were measured at the Marsh Landing Weather Station operated as part of the GCE-LTER program. Wind stress was computed following Large et al. (1994) and decomposed into alongshore and cross-shore components.

## Ocean Model

We used outputs from an ocean model based on the Finite Volume Community Ocean Model (FVCOM; Chen et al. 2006a,b, 2007, 2008). The model implementation to the Altamaha River estuary is described in detail in Wang et al.

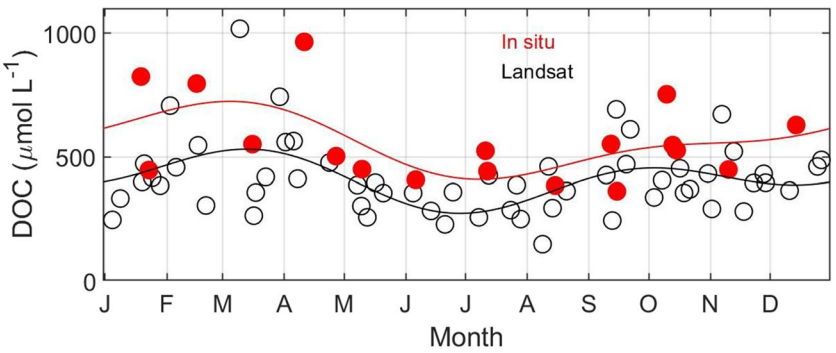


**Fig. 4** Time series of DOC concentration (µmol $L^{-1}$) at the Altamaha River (at station shown by red circle in Fig. 1) based on in situ (red) and Landsat (black) observations. Red and black lines show seasonal cycles, estimated using two harmonics

(2017). Briefly, the model uses an unstructured grid that includes wetting and drying capability. Model resolution is 30–70 m in tidal creeks, around 100–200 m in the main estuarine channels, and increases progressively to about 1.2 km near the model boundary. The model is forced by Altamaha River discharge obtained from the USGS gauge at Doctortown, GA, wind forcing from NOAA's National Data Buoy Center buoy 41,008 and by eight tidal constituents extracted from the Oregon State University tidal model (Egbert and Erofeeva 2002). Wang et al. (2017) also included a small freshwater input at the head of Sapelo Sound equivalent to 5% of the Altamaha River discharge, which minimized the bias between observed and modeled salinity at Sapelo Sound. Additional details about the model implementation can be found in Wang et al. (2017). The model simulation focused on 2008, a year characterized by normal river discharge. Even though that period does not match the period covered by Landsat observations, model outputs are useful to help quantify the effects of different forcing on variability in the estuary.

## Results

### Distribution and Variability of Dissolved Organic Carbon in the Estuary

The Altamaha River has a major influence on salinity distribution in the estuary (Fig. 1; Di Iorio and Castelao 2013; Wang et al. 2017). The long-term average of Landsat observations reveals that it also has a major effect on DOC concentrations (Fig. 5a). DOC content is higher in the river, decreasing progressively in the Altamaha Sound toward the ocean. A similar pattern is also observed in Doboy and Sapelo Sounds (see Fig. 1 for locations), although average DOC concentrations in those sounds are generally smaller than in the Altamaha River and Sound. The area near the head of Sapelo Sound is also characterized by increased DOC concentrations. That is consistent with Medeiros et al. (2015) and Letourneau et al. (2021) in situ observations, who showed high DOC content in that region. The Altamaha Sound and the upper halves of Doboy and Sapelo Sounds are also characterized by increased variability in DOC concentrations (Fig. 5b). High standard deviations are especially observed in narrow channels and creeks connecting the main channels. The average and the standard deviation of DOC concentrations in the estuary (shown in Fig. 5) are spatially correlated to each other ($r=0.49$, $p<0.001$), so that increased standard deviation in narrow channels and creeks is likely related to the observed increased concentrations in those regions. Variability may also be influenced by other factors, such as inputs from the surrounding marshes. Over the shelf, increased variability is observed especially near the mouth of the Altamaha Sound.

Landsat observations were decomposed into empirical orthogonal functions (EOFs) to extract the dominant modes of variability in the system. Both modes shown here are statistically significant at the 95% level (Overland and

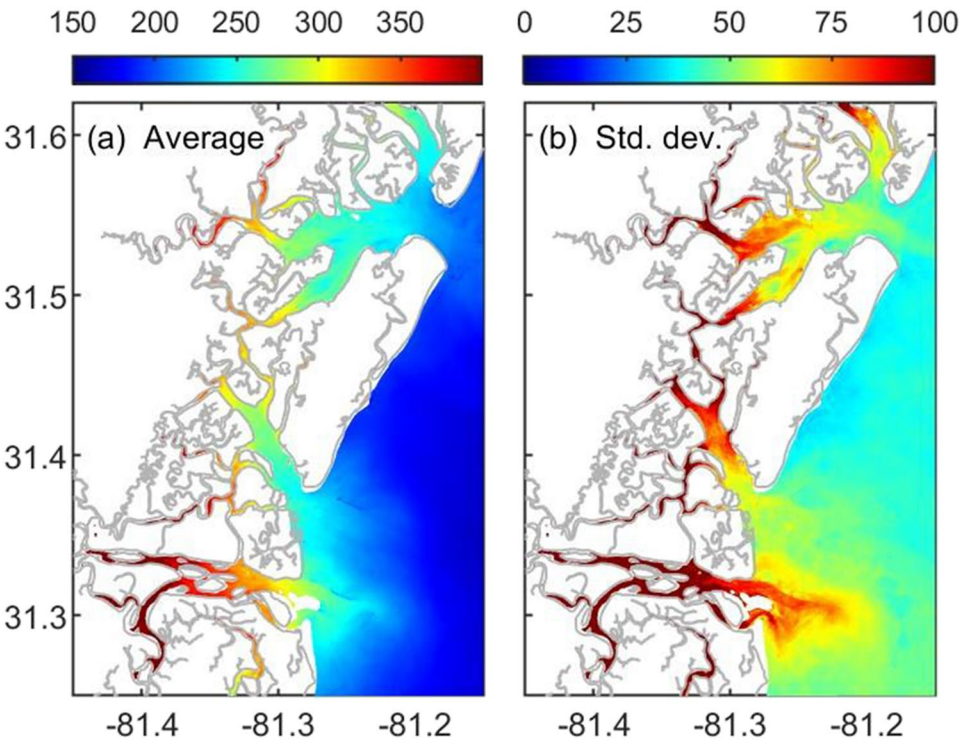


**Fig. 5** Long-term (2013–2023) (a) average and (b) standard deviation of DOC concentration (μmol $L^{-1}$) in the Altamaha River estuary from Landsat observations

Preisendorfer 1982). The first mode explains 62.7% of the total variance, and it is characterized by an increased signal in the Altamaha River and Sound extending offshore into the coastal ocean, and in the upstream halves of Doboy and Sapelo Sounds (Fig. 6a), closely resembling the pattern observed in the DOC standard deviation field (Fig. 5b). At Doboy Sound and in the adjacent costal ocean, the mode explains up to 80% of the local variance (Fig. 6c). The amplitude time series for mode 1 is characterized by two peaks, one in spring and another during fall (Fig. 6f), indicating that DOC concentrations increase throughout the estuary during those seasons. The amplitude time series is negative during summer and winter, indicating that the mode captures a decrease in DOC concentrations in the estuary during those seasons compared to the long-term average. Note that increased DOC concentrations in spring and fall with decreased values during summer are also observed in the time series of in situ observations in the Altamaha River (red circles in Fig. 4; Medeiros 2022). The amplitude time series for individual years indicates large differences (Fig. 6e), with substantial increases in some years, such as in the springs of 2016, 2018, and 2022 and the falls of 2014, 2017, and 2021.

The second EOF mode is characterized by a zero crossing near the mouth of each sound (Fig. 6b), capturing an out-of-phase response between the estuary and the coastal ocean.

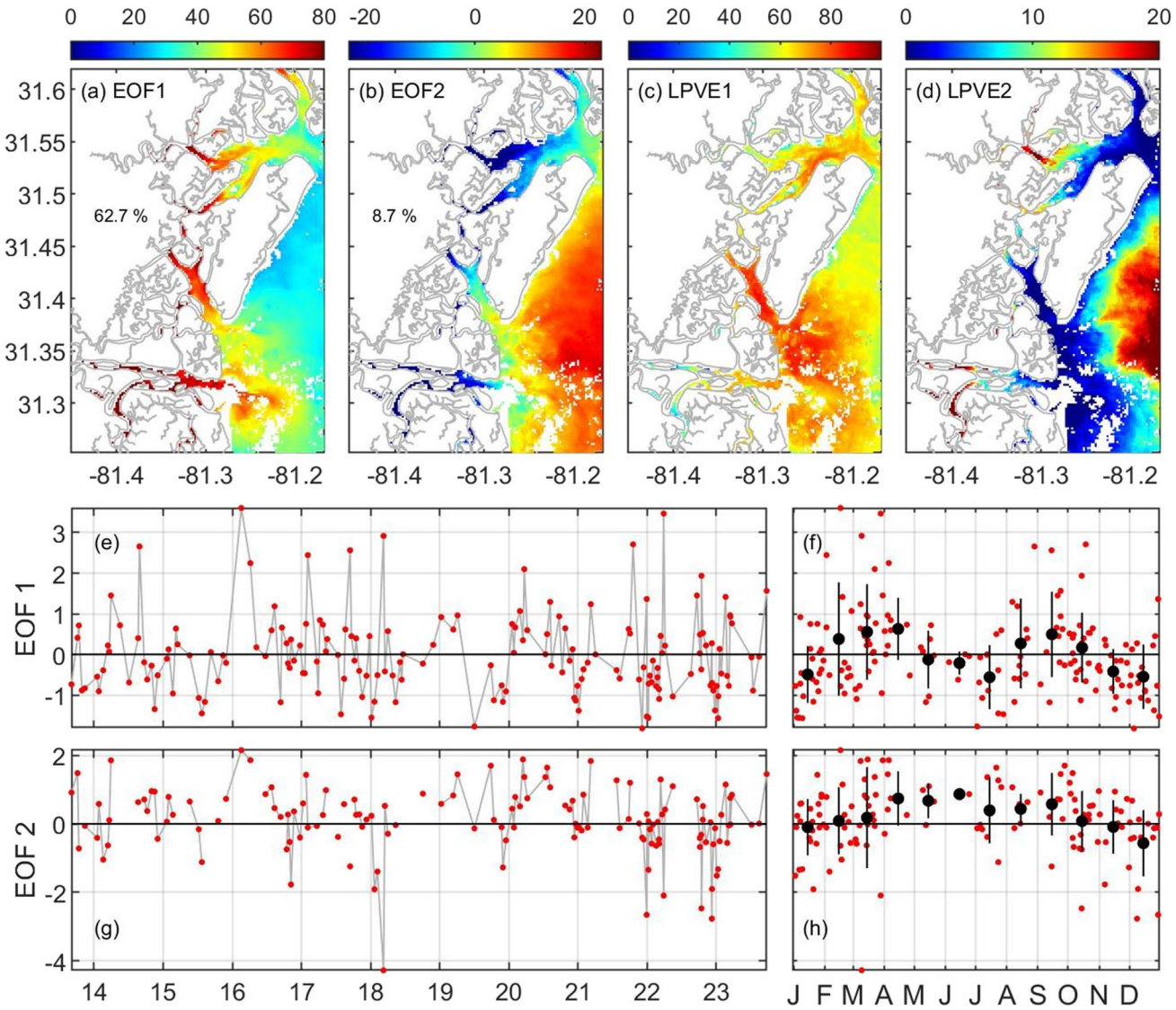


**Fig. 6** (a) EOF 1 and (b) EOF 2 of DOC concentration from Landsat in the Altamaha River estuary. The fraction of the total variance explained by each mode is shown. Amplitude time series for each mode are shown in panels (e) and (g), while their seasonal evolution is shown in panels (f) and (h). Averages ± 1 standard deviation for each month are shown in black. The local percentage of variance explained (LPVE) by EOF 1 and 2 are shown in panels (c) and (d), respectively

The amplitude time series (Fig. 6g, h) indicates that the mode captures an increase in DOC concentrations over the shelf during summer and a decrease during winter, while the opposite is true upstream in the estuary. Although the mode explains a relatively large fraction of the local variance over the shelf, exceeding 20% in some areas, it explains very little of the variance in the estuary, except in a few isolated spots upstream in the Altamaha and Sapelo Sounds (Fig. 6d).

## Drivers of Estuarine Variability

To quantify the relative importance of some of the main physical drivers of DOC variability in the estuary, we compared time series of various forcings and DOC concentrations from Landsat. A challenging aspect of the analysis is that Landsat data are not regularly spaced in time. There are only 170 satellite images available during the ~ 10 years analyzed here, with more observations being available during winter and less during summer because of variability in cloud cover and/or sun glint contamination (Fig. 2). To investigate how this may affect results, we first analyzed the relationship between forcing and salinity variability in the hydrodynamic model. We computed 2 sets of correlation coefficients: one using the full model output at 1 h interval, and another where we selected 170 snapshots of model output matching the same day of the year and tidal phase of the Landsat data. We computed correlations between river discharge and modeled surface salinity, and between surface elevation and surface salinity. Because time series are dominated by seasonal variability, we first removed the seasonal cycle (annual and semiannual harmonics) to focus on anomalies. When comparing salinity with river discharge, the time series were also low-pass filtered (half-power point of 40 h; Mooers et al. 1968) to suppress tidal and inertial oscillations. We computed the correlation coefficients between river discharge and salinity using a lag of 8 days, consistent with the average lag between river discharge and salinity variability in the system based on observations (Di Iorio and Castelao 2013). Using a lag of 6 or 10 days produces qualitatively similar results. For surface elevation and salinity, no lag was used.

As expected, anomalies in river discharge and anomalies in surface salinity were found to be highly correlated over much of the estuary, but especially in the Altamaha and Doboy Sounds and the adjacent coastal ocean and upstream in Sapelo Sound (Fig. 7a). Correlations were mostly negative, indicating that increases in river discharge resulted in widespread freshening in the estuary, which is consistent with observations (Di Iorio and Castelao 2013). Correlations between surface elevation and surface salinity anomalies, on the other hand, are positive and highest in the coastal ocean near the mouth of the Altamaha Sound (Fig. 7c), as low-salinity water from the estuary is transported back and forth into the coastal ocean due to tidal forcing. Correlations are also positive over most of Sapelo Sound, as freshwater introduced at the head of the sound is transported downstream during low tide and upstream during high tide. Negative correlations were observed in the northernmost channel of the model domain, at 81.2°W, 31.6°N. This is most likely an artifact due to the fact that no freshwater input was considered in the model at the head of that channel as a boundary condition. As a result, low-salinity water found in the coastal ocean is transported into the channel during high tides, resulting in negative correlation. In reality, that channel is connected to an adjacent sound to the north of the model domain via the Intracoastal Waterway and is thus supplied with freshwater from upstream. Quantitatively similar results were obtained when model results were subsampled to match the temporal characteristics of the satellite observations (Fig. 7b, d), indicating that the statistical relationship between forcing and salinity variability can be reliably obtained with the subsampled data. This suggests that Landsat data can be used to quantify the relationship between forcing and variability in the estuary.

Time series of DOC concentration from Landsat at each satellite pixel were reconstructed using a multiple linear regression analysis to isolate the relative contribution of various forcing to DOC variability in the estuary, following Belem et al. (2013). We included annual and semiannual harmonics ($2\pi/365.25$ and $4\pi/365.25$ days, respectively), and time series of anomalies of river discharge (with an 8-day lag), sea surface elevation, and alongshore and cross-shore wind stress. Anomalies of each forcing were constructed by removing the respective seasonal cycles. Additionally, each of these forcing was first normalized by their respective standard deviations (Table 1). The resulting forcings are uncorrelated with each other, except for the alongshore and cross-shore wind stress anomalies, which are weakly correlated (Table 2). We note that using a linear model is a simplification and it may not fully capture potential nonlinear relationships between the multiple forcing and DOC variability. Maps of the regression coefficients are shown in Fig. 8 and are related to the contribution of each forcing to total variability in DOC concentration in the estuary. The annual and semiannual harmonics are the largest terms, although their relative contributions vary spatially. The annual harmonic is particularly important in the Altamaha River and Sound, peaking in March/April (Fig. 8a, e). The semiannual harmonic is important throughout the estuary and near the mouth of Altamaha Sound extending into the shelf (Fig. 8b). The phase of the semiannual harmonic (i.e., two peaks per year) indicates a peak in March/April (Fig. 8f) and another peak 6 months later. That is consistent with the dominant mode of variability in the system as identified by the EOF analysis (Fig. 6a, f). The regression

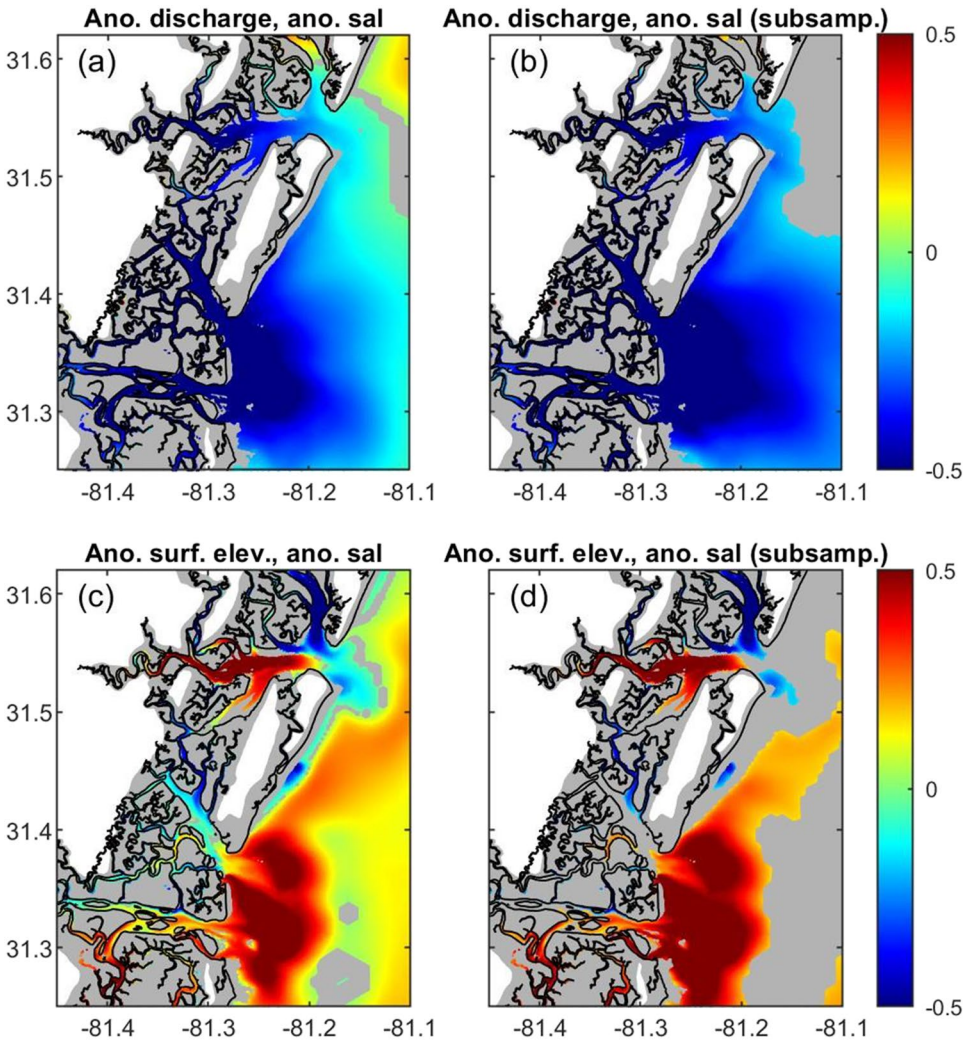


**Fig. 7** Correlation coefficients based on ocean model outputs for (a, b) anomaly (i.e., seasonal cycle removed) in river discharge (with an 8-day lag) and anomaly in salinity and for (c, d) anomaly in surface elevation and anomaly in salinity. Correlations were computed using the full model output (1 model output per hour; a, c), or using model output subsampled to match the characteristics of the satellite observations (i.e., same day of the year and tidal phase; b, d). Only statistically significant coefficients ($p < 0.05$) are shown

**Table 1** Standard deviation of various forcing used in multiple linear regression model

| Variable (anomalies) | Standard deviation |
|---|---|
| Altamaha River discharge | 316 $m^3s^{-1}$ |
| Surface elevation | 0.74 m |
| Alongshore wind stress | 0.013 Pa |
| Cross-shore wind stress | 0.010 Pa |

coefficient for the river discharge term is positive over most of the region (Fig. 8c) and indicates that a pulse in river discharge equivalent to one standard deviation (Table 1) is accompanied by an increase in DOC concentration of about 20 µmol $L^{-1}$ over most of the region. A comparable change in DOC concentration is observed in response to surface elevation variability near the mouth of the Altamaha and Sapelo Sounds (Fig. 8d). Because

**Table 2** Cross-correlation among the various forcing used in multiple linear regression model. The seasonal cycle has been removed from all variables

| **Variable (anomalies)** | Altamaha River discharge | Surface elevation | Alongshore wind stress | Cross-shore wind stress |
|---|---|---|---|---|
| Altamaha River discharge | 1 | −0.03 | −0.01 | 0.09 |
| Surface elevation | - | 1 | 0.00 | 0.03 |
| Alongshore wind stress | - | - | 1 | 0.24* |
| Cross-shore wind stress | - | - | - | 1 |

*Significant at the 95% confidence level

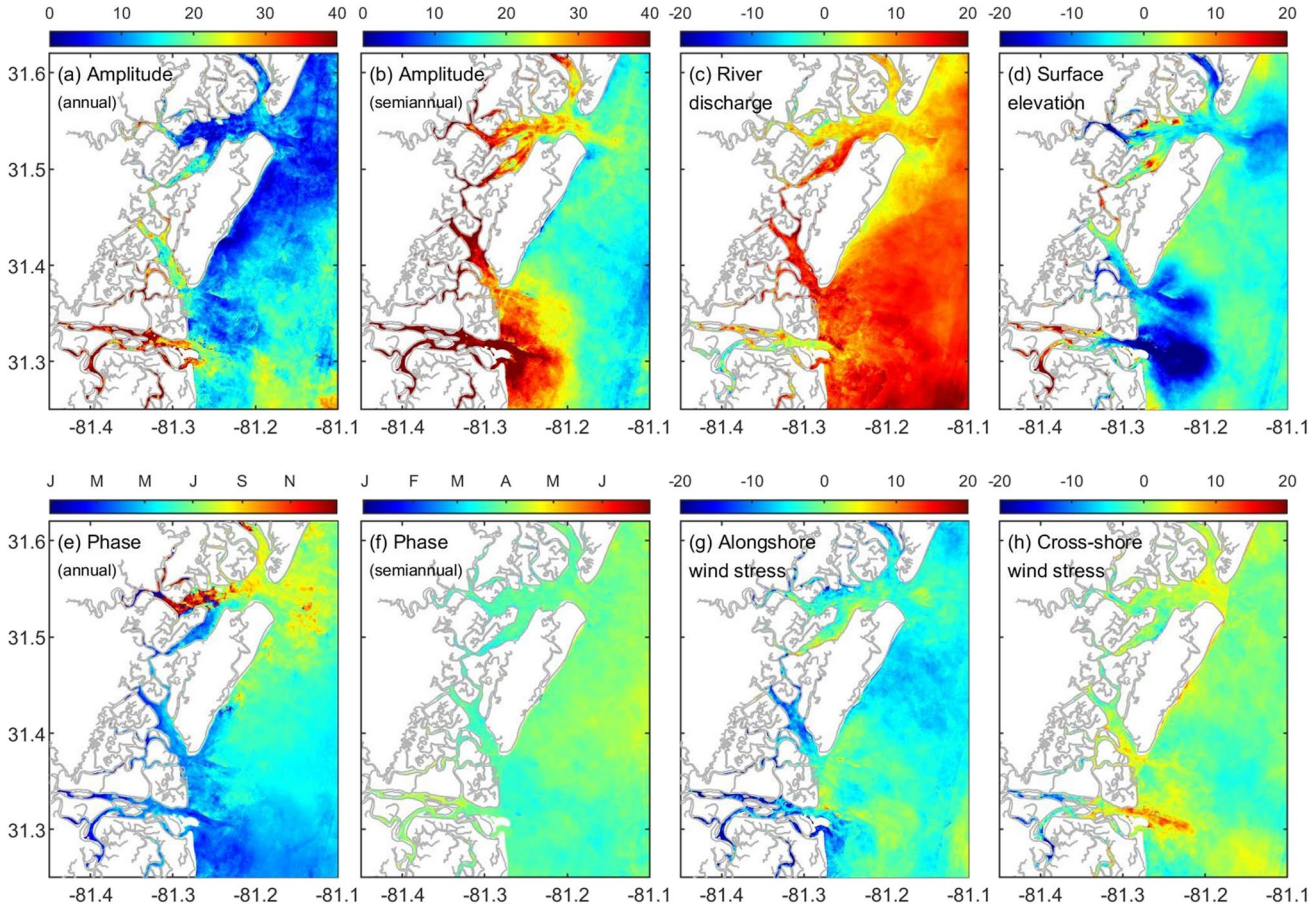


**Fig. 8** Normalized coefficients from a multiple linear regression analysis between DOC observations from Landsat and (a, b, e, f) harmonics with two different periods (365.25 and 365.25/2 days), anomalies (i.e., seasonal cycle removed) in (c) river discharge (with an 8-day lag), (d) surface elevation, and (g) alongshore and (h) cross-shore wind stress. The time series of each forcing have been divided by their respective standard deviations (shown in Table 1) and the regression coefficients have been multiplied by those same standard deviations. As a result, the time series of the various forcing are non-dimensional, while the normalized regression coefficients have units of μmol $L.^{-1}$

variability in surface elevation is dominated by high-frequency motion (i.e., tides), these changes in DOC concentration are short-lived and mostly associated with estuarine water being transported out of and back into the estuary due to tidal forcing. Variability in DOC concentration in response to changes in surface elevation is also observed near the head of Sapelo Sound, and in some of the channels connecting Doboy and Altamaha Sounds (Fig. 8d). Lastly, the influence of winds is substantially smaller over most regions (Fig. 8g, h), except near the mouth of the Altamaha Sound. In that case, positive cross-shore winds (i.e., blowing out of the estuary) are associated with increased DOC concentration over the shelf.

## Carbon Input Associated with Hurricane Irma

The Altamaha River estuary has been impacted by the passage of multiple hurricanes over the last few years (Medeiros 2022). In 2017, in particular, Hurricane Irma resulted in substantial storm surge (Fig. 9a) and increased precipitation in the estuary (Medeiros 2022). In situ observations collected at 15 stations a few weeks after the passage of the hurricane revealed a large input of DOC to the system (Letourneau et al. 2021). A mostly clear-sky Landsat image is available about 3 days after the passage of the storm, which indicated that DOC anomalies (i.e., deviations from the seasonal cycle) were large and positive over the entire estuarine region extending into the shelf near the mouth of the Altamaha Sound (Fig. 9b). The image was obtained during low-tide conditions, which may have contributed to the offshore transport of estuarine waters and increased DOC anomalies over the shelf (see Fig. 8d). A sharp front was observed over the shelf near the Altamaha Sound mouth (Fig. 9c), with large DOC differences occurring over a scale of less than 100 m (Fig. 9d).

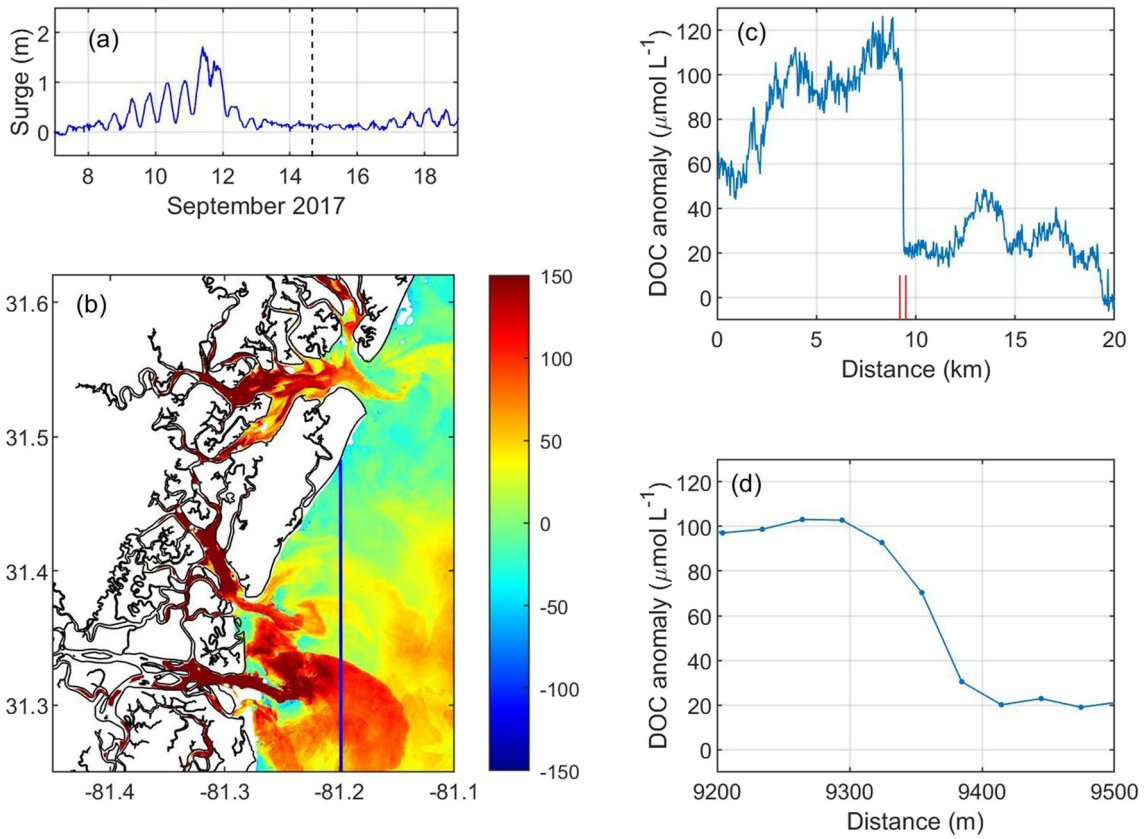


**Fig. 9** (a) Time series of sea level anomaly (i.e., removing predicted tides) at Fort Pulaski, GA in September 2017 during the passage of Hurricane Irma. Dashed line shows timing of Landsat observation. (b) DOC anomaly (i.e., deviation from seasonal cycle) in the Altamaha River estuary approximately 3 days after the passage of Hurricane Irma (in μmol $L.^{-1}$). (c) DOC anomaly along the transect shown in blue in panel (b). The same data is shown in panel (d) but focusing on the front. Vertical red lines in panel (c) indicate the window shown in panel (d)

We used this Landsat image to quantify the amount of DOC introduced into the estuary associated with the passage of Hurricane Irma. Previous studies have shown that stratification in the estuary during low discharge conditions, such as those observed during this period (Medeiros 2022), is generally weak (Di Iorio and Kang 2007). Thus, we assumed that DOC concentrations are depth independent. Observations are not available in several regions upstream in the estuary due to cloud coverage and/or sun glint contamination (areas with missing data in Fig. 9b). We filled those gaps in observations using the average DOC anomaly in the estuary during that time (155 μmol $L^{-1}$). Note that this likely represents an underestimation of actual DOC anomalies, since concentrations generally increase upstream in the estuary (Medeiros et al. 2015; Letourneau et al. 2021). With these assumptions, the total DOC content anomaly in the estuary could be estimated by first multiplying the area of each pixel in the Landsat image by the local water depth, yielding a volume for each pixel. That volume was then multiplied by the local DOC anomaly. Results were then integrated over the entire estuary, yielding the total DOC content in the estuary that was observed in excess of the seasonal pattern. The calculation revealed that the passage of the hurricane was followed by the addition of 1.88 Gg of DOC to the estuary. For comparison, if we assume average river discharge and average DOC concentration for the Altamaha River, this is equivalent to the amount of DOC added to the estuary by the river during a period of about 9 days.

## Discussion

Estuaries are highly dynamic systems where variability occurs on a continuum of scales (Wolfe and Kjerfve 1986), both temporally and spatially. This makes investigating variability in those systems challenging, as traditional sampling that can resolve temporal variability well (e.g., moorings) is generally not well-suited to resolve small-scale spatial variability. The recent availability of high-resolution observations from satellites can be used to fill that gap. Cao and Tzortziou (2021) showed, for example, that Landsat observations can be used to estimate DOC concentrations in estuaries in high

resolution over long periods of time. Given that inputs from rivers are an important source of DOC to estuaries (Spencer et al. 2012), DOC concentrations are often correlated with salinity in those systems (e.g., Harvey and Mannino 2001). The relationship is often nonlinear and can break down in several instances, as there are sources (e.g., marsh-derived inputs, phytoplankton blooms; Tzortziou et al. 2008; Osburn et al. 2015; Moran et al. 2016) and sinks (e.g., bio- and photo-chemical degradation, flocculation; Asmala et al. 2014; Seidel et al. 2016) of DOC that are uncorrelated to salinity variability. Despite these, several studies have shown that ocean color data can provide useful information about variability in river-influenced waters in different coastal settings (Fournier et al. 2015; da Silva and Castelao 2018). Correlations between DOC and salinity in the Altamaha River estuary (Letourneau and Medeiros 2019) and in many other estuaries worldwide (e.g., Harvey and Mannino 2001; Abril et al. 2002; Callahan et al. 2004; Sharp et al. 2009) are generally statistically significant, indicating that Landsat data can also provide information about variability in estuarine physical properties.

Our use of Landsat data revealed that DOC concentrations in the Altamaha River decrease progressively toward the ocean, in agreement with Letourneau et al. (2021) in situ observations, and that variability is dominated by the seasonal cycle, in particular the semiannual harmonic. The increase in DOC concentration in March/April coincides with the seasonal peaks in river discharge (Di Iorio and Kang 2007) and in DOC flux from the Altamaha River (Medeiros et al. 2017), indicating the importance of allochthonous inputs to the estuary. A second seasonal increase is observed 6 months later, in September/October. That can be at least partially related to DOC leached from marsh plants, which is often observed during fall senescence (McDowell 1985; Singh et al. 2014; Schiebel et al. 2018), although it may also be related to a secondary peak in river discharge that is sometimes observed in the fall (Blanton and Atkinson 1983). In contrast to the pattern of variability observed in a small bay in Chesapeake Bay by Cao and Tzortziou (2021), who reported an increase during summer, DOC concentrations in the Altamaha River estuary during summer are at a local minimum, and increases in DOC concentration during that time are restricted to the shelf.

Over shorter time scales, within the "weather band", the analyses conducted here allowed for the quantification of spatial variability in the relative contributions of different forces to DOC variability in the system. The regression model (Fig. 8) only includes physical forcing associated with advection and mixing in the estuary, including river discharge, tidal variability, and winds. As such, many processes that are known to drive DOC variability in estuaries, such as inputs from phytoplankton (Cifuentes and Eldridge 1998), bio- and photo-chemical degradation (Moran et al. 1999; Raymond and Bauer 2000), and flocculation (Asmala et al. 2014), are not explicitly represented, except to the extent that they are captured by the annual and semiannual harmonics. The model revealed that winds make a small contribution to DOC variability in the system, except very near the mouth of the Altamaha Sound, presumably associated with increases in offshore transport of estuarine waters with high DOC content due to intensified offshore winds. Pulses in river discharge, on the other hand, are directly related to DOC concentration over most of the estuary and the adjacent coastal ocean. This is consistent with previous studies that have shown that DOC concentration and the composition of the dissolved organic matter pool in the estuary are influenced by variability in river discharge (Medeiros et al. 2015; Letourneau and Medeiros 2019). Anomalies in river discharge have a small influence on anomalies in DOC concentration from Landsat at the Altamaha Sound (Fig. 8c), however, which is surprising. In situ observations and modeling results have revealed that river discharge and salinity are correlated in this sound (Di Iorio and Castelao 2013; Wang et al. 2017; see also Fig. 7). Both river discharge (Di Iorio and Castelao 2013) and DOC concentrations at the Altamaha Sound (Fig. 8a) have a clear seasonal cycle. Thus, it is possible that the expected correlation between river discharge and DOC concentration at the Altamaha Sound occurs mostly at the seasonal band, and that any remaining correlation between anomalies may have been obscured by noise in the satellite data.

It is also surprising that the influence of surface elevation variability on DOC concentrations is mostly restricted to near the mouth of the Altamaha and Sapelo Sounds. Previous studies in the region (e.g., Martineac et al. 2021) and in other estuaries (e.g., Tzortziou et al. 2008) have shown that DOC concentrations and dissolved organic matter composition can vary in response to tidal forcing, with DOC concentration generally increasing during low-tide conditions. The signature of marsh-derived inputs in the estuary is only seen upstream in Sapelo Sound and in some of the channels and creeks connecting the Altamaha and Doboy Sounds (where the regression coefficient in Fig. 8d is large and negative). The in situ data used for algorithm calibration was collected during 4 sampling surveys under high tide conditions (Letourneau et al. 2021), and as such it was not possible to use only in situ and satellite data match ups from the same tidal phase when calibrating the algorithm. This may have impacted the algorithm's ability to capture the expected increase in DOC content during low-tide conditions as in Cao and Tzortziou (2021). We note that the range of variability in DOC concentrations in the estuary over seasonal and spatial scales is larger than the range of variability due to tides (Letourneau et al. 2021; Martineac et al. 2021), so we expect uncertainties in the algorithm due to differences in tidal phase between in situ and satellite data

to be comparatively small. Future in situ sampling designed to match the timing of Landsat data, thus capturing the same tidal phase, can be used to quantify this uncertainty and refine the algorithm. Despite this, the root-mean-square error and the mean average percent difference for the algorithm used here are comparable to those reported by Cao and Tzortziou (2021). Additionally, the algorithm is capable of reproducing DOC variability of an independent data set (i.e., not used for algorithm calibration) collected over multiple years at the Altamaha River (Medeiros 2022), just upstream of the head of Altamaha Sound (see Fig. 4). Although the algorithm can nicely capture the seasonal evolution of DOC in the river, concentrations are generally smaller than those from in situ observations. Some of the in situ and satellite observations were collected in different years, so part of these differences is likely simply a result of temporal variability in the system. In situ concentrations at this upstream site can be quite high, however, often exceeding the range of in situ observations available for algorithm calibration. Therefore, it is also possible that the algorithm underestimates DOC concentrations in this high-concentration limit. Additional in situ observations spanning a larger range of DOC concentrations in the estuary (and collected at the same tidal phase of Landsat data) are needed to further refine the algorithm. We note that we did not use Sentinel-2 observations in this study because the time interval between the available in situ sampling and satellite passages with cloud-free data was larger, sometimes exceeding 10 days. Obtaining in situ data matching Sentinel-2 observations would allow for an algorithm to be calibrated for those measurements, which would increase the number of satellite-derived DOC observations available in the estuary substantially.

Although the observations do not allow for fully resolving interannual variability, the long-term time series of Landsat data can capture events of interest, such as a large increase in DOC concentrations during early 2016, which may be related to an El Niño event (Santoso et al. 2017), which generally results in increased discharge at the Altamaha River (Clark II et al. 2014). Landsat observations may be particularly useful to investigate estuarine variability following extreme events such as the passage of tropical storms and hurricanes, when in situ sampling can be logistically difficult and unsafe to obtain. This is important, because the frequency of extreme weather events may be increasing in the southeastern U.S. (Paerl et al. 2018), which may result in increased DOC transfer to the ocean (Rudolph et al. 2020). In fall 2017, Landsat data was available about 3 days after the passage of Hurricane Irma, providing useful information about the estuarine response to this extreme event. We were able to quantify a large input of DOC to the system (which is consistent with in situ DOC data collected about 1 month after the passage of the storm; Letourneau et al. 2021; Medeiros 2022) and the offshore transport of DOC-rich waters into the shelf. The temporal availability of Landsat images is low, however, because of coarse temporal revisit and cloud and sun glint contamination (Cao and Tzortziou 2021). Therefore, observations following extreme events will only be available in some instances.

Our focus on this study was the estuarine region, which is characterized by complex coastline and small spatial scales of variability, making the use of high-resolution Landsat data advantageous (Cao and Tzortziou 2021). Only data from the estuary was used to parameterize the relationship between the satellite measurements of Rrs and in situ DOC concentration in Eq. (1). As a result, DOC estimates over the shelf, especially away from the mouths of each of the estuarine sounds, are likely to be more uncertain and characterized by larger errors. Studies focusing on the shelf, where spatial scales of variability are comparatively larger, may benefit from the use of observations from other satellites/sensors with a shorter revisit time, such as MERIS (Cao et al. 2018), MODIS (Fichot et al. 2014), or SeaWiFS (Mannino et al. 2016). We also note that uncertainties in the algorithm may exist due to interference of particulate organic carbon content or sediments in the satellite signals (Salisbury et al. 2011; Yamaguchi et al. 2013). Despite all the challenges described above, Landsat observations can provide complementary information to indispensable in situ data, including informing on the dominant scales of variability in narrow estuaries, capturing the occurrence of sharp fronts that would be difficult to observe with traditional in situ observations alone, and providing observations when in situ data are difficult to obtain, such as following extreme events. It can also provide guidance for in situ observational programs, such as informing the selection of locations for mooring deployments and shipboard surveys, as Landsat data can be used to identify a priori regions that are more strongly influenced by river discharge, tidal variability, and wind forcing, as well as regions characterized by large variability at seasonal scales. The algorithm provided accurate results for two different systems, Chesapeake Bay (Cao and Tzortziou 2021) and the Altamaha River estuary, suggesting that it can be used to investigate variability in other estuaries worldwide. The relationship between optical properties and DOC concentrations often varies between regions (Mannino et al. 2008), however, so it is important that the algorithm be calibrated with local data.

**Acknowledgements** We thank the two anonymous reviewers for their constructive comments and suggestions, which resulted in an improved manuscript.

**Funding** This work was supported by the National Science Foundation through the Georgia Coastal Ecosystems LTER Program (OCE-1832178) and grant OCE-1902131. This is UGAMI contribution number 1129.

**Data Availability** Satellite data used in this study are publicly available at https://earthexplorer.usgs.gov. In situ data used can be found in Letourneau et al. (2021) and Medeiros (2022) and at the GCE-LTER data portal (https://gce-lter.marsci.uga.edu/portal).

## Declarations

**Conflict of Interest** The authors declare no competing interests.

## References

Abril, G., M. Nogueira, H. Etcheber, G. Cabeçadas, E. Lemaire, and M. Brogueira. 2002. Behavior of organic carbon in nine contrasting European estuaries. *Est. Coast. Shelf Sci.* 54: 241–262.

Alber, M., D. Reed, and K. McGlathery. 2013. Coastal long term ecological research: Introduction to the special issue. *Oceanography* 26 (3): 14–17.

Asmala, E., D.G. Bowers, R. Autio, H. Kaartokallio, and D.N. Thomas. 2014. Qualitative changes of riverine dissolved organic matter at low salinities due to flocculation. *Journal of Geophysical Research: Biogeosciences* 119: 1919–1933. https://doi.org/10.1002/2014JG002722.

Bauer, J., W.J. Cai, P. Raymond, T.S. Bianchi, C.S. Hopkinson, and P.A.G. Regnier. 2013. The changing carbon cycle of the coastal ocean. *Nature* 504: 61–70.

Belem, A.L., R.M. Castelao, and A.L. Albuquerque. 2013. Controls of subsurface temperature variability in a western boundary upwelling system. *Geophysical Research Letters* 40: 1362–1366. https://doi.org/10.1002/grl.50297.

Blanton, J.O., and L.P. Atkinson. 1983. Transport and fate of river discharge on the continental shelf of the southeastern United States. *Journal of Geophysical Research* 88: 4730–4738.

Callahan, J., M. Dai, R. Chen, X. Li, Z. Lu, and W. Huang. 2004. Distribution and dissolved organic matter in the Pearl River Estuary. *China. Mar. Chem.* 89: 211–224.

Canuel, E.A., and A.K. Hardison. 2016. Sources, ages, and alteration of organic matter in estuaries. *Annual Review of Marine Science* 8: 409–434.

Canuel, E., S. Cammer, H. McIntosh, and C. Pondell. 2012. Climate change impacts on the organic carbon cycle at the land-ocean interface. *Ann. Rev. Earth Planet. Sci.* 40: 685–711.

Cao, F., and M. Tzortziou. 2021. Capturing dissolved organic carbon dynamics with Landsat-8 and Sentinel-2 in tidally influenced wetland-estuarine systems. *Sci. Tot. Environ.* 777: 145910.

Cao, F., M. Tzortziou, C. Hu, A. Mannino, C.G. Fichot, R. Del Vecchio, R.G. Najjar, and M. Novak. 2018. Remote sensing retrievals of colored dissolved organic matter and dissolved organic carbon dynamics in North American estuaries and their margins. *Remote Sensing of Environment* 205: 151–165.

Chen, C., R.C. Beardsley, and G. Cowles. 2006b. An unstructured grid, finite-volume coastal ocean model (FVCOM) system: Special issue entitled "Advances in Computational Oceanography." *Oceanography* 19 (1): 78–89.

Chen, C., H. Huang, R.C. Beardsley, H. Liu, Q. Xu, and G. Cowles. 2007. A finite-volume numerical approach for coastal ocean circulation studies: Comparisons with finite-difference models. *Journal of Geophysical Research* 112: C03018.

Chen, C., J. Qi, C. Li, R.C. Beardsley, H. Lin, R. Walker, and K. Gates. 2008. Complexity of the flooding/drying process in an estuarine tidal-creek salt-marsh system: An application of FVCOM. *Journal of Geophysical Research* 113: C07052.

Cifuentes, L., and P. Eldridge. 1998. A mass- and isotope-balance model of DOC mixing in estuaries. *Limnology and Oceanography* 43: 1872–1882.

Clark, C., II., G. Nnaji, and W. Huang. 2014. Effects of El Niño and La Niña sea surface temperature anomalies on annual precipitations and streamflow discharges in southeastern United States. *Journal of Coastal Research* 68: 113–120.

da Silva, C.E., and R.M. Castelao. 2018. Mississippi River plume variability in the Gulf of Mexico from SMAP and MODIS-Aqua observations. *Journal of Geophysical Research: Oceans* 123: 6620–6638.

Di Iorio, D., and R.M. Castelao. 2013. The dynamical response of salinity to freshwater discharge and wind forcing in adjacent estuaries on the Georgia coast. *Oceanography* 26: 44–51.

Di Iorio, D., and K.R. Kang. 2007. Variations of turbulent flow with river discharge in the Altamaha River Estuary, Georgia. *Journal of Geophysical Research* 112: C05016. https://doi.org/10.1029/2006JC003763.

Egbert, G.D., and S.Y. Erofeeva. 2002. Efficient inverse modeling of barotropic ocean tides. *Journal of Atmospheric and Oceanic Technology* 19: 183–204. https://doi.org/10.1175/1520-0426(2002)019%3c0183:EIMOBO%3e2.0.CO;2.

Fichot, C.G., S.E. Lohrenz, and R. Benner. 2014. Pulsed, cross-shelf export of terrigenous dissolved organic carbon to the Gulf of Mexico. *Journal of Geophysical Research: Oceans* 119: 1176–1194.

Fournier, S., B. Chapron, J. Salisbury, D. Vandemark, and N. Reul. 2015. Comparison of spaceborne measurements of sea surface salinity and colored detrital matter in the Amazon plume. *Journal of Geophysical Research: Oceans* 120: 3177–3192.

Harvey, H.R., and A. Mannino. 2001. The chemical composition and cycling of particulate and macromolecular dissolved organic matter in temperate estuaries as revealed by molecular organic tracers. *Org. Goechem.* 32: 527–542.

Hedges, J.I., R.G. Keil, and R. Benner. 1997. What happens to terrestrial organic matter in the ocean? *Organic Geochemistry* 27: 195–212.

Kirwan, M.L., and J.P. Megonigal. 2013. Tidal wetland stability in the face of human impacts and sea-level rise. *Nature* 504 (7478): 53–60.

Large, W.G., J.C. McWilliams, and S.C. Doney. 1994. Oceanic vertical mixing: A review and a model with a nonlocal boundary layer parameterization. *Reviews of Geophysics* 32: 363–403.

Lee, T.N., and D.A. Brooks. 1979. Initial observations of current, temperature and coastal sea level response to atmospheric and Gulf Stream forcing on the Georgia shelf. *Geophysical Research Letters* 6: 321–324.

Letourneau, M.L., and P.M. Medeiros. 2019. Dissolved organic matter composition in a marsh-dominated estuary: Response to seasonal forcing and to the passage of a hurricane. *Journal of Geophysical Research: Biogeoscience* 124 (6): 1545–1559.

Liu, Q., D. Pan, Y. Bai, K. Wu, C.-T.A. Chen, Z. Liu, and L. Zhang. 2014. Estimating dissolved organic carbon inventories in the East China Sea using remote-sensing data. *J. Geophys. Res. Oceans* 119: 6557–6574. https://doi.org/10.1002/2014JC009868.

MacCready, P., and W.R. Geyer. 2010. Advances in estuarine physics. *Annual Review of Marine Science* 2: 35–58.

Mannino, A., M.E. Russ, and S.B. Hooker. 2008. Algorithm development for satellite-derived distributions of DOC and CDOM in the

U.S. Middle Atlantic Bight. *J. Geophys. Res.* 113: C07051. https://doi.org/10.1029/2007JC004493.

Mannino, A., S.R. Signorini, M.G. Novak, J. Wilkin, M.A.M. Friedrichs, and R.G. Najjar. 2016. Dissolved organic carbon fluxes in the Middle Atlantic Bight: An integrated approach based on satellite data and ocean model products. *Journal of Geophysical Research. Biogeosciences* 121: 312–336. https://doi.org/10.1002/2015JG003031.

Martineac, R.P., A.V. Vorobev, M.A. Moran, and P.M. Medeiros. 2021. Assessing the contribution of seasonality, tides, and microbial processing to dissolved organic matter composition variability in a Southeastern U.S. Estuary. *Front. Mar. Sci.* 8: 781580.

Martineac, R.P., R.M. Castelao, and P.M. Medeiros. 2024. Seasonal and interannual variability in the distribution and removal of terrigenous dissolved organic carbon in the Amazon River plume. *Global Biogeochemical Cycles* 38: e2023GB007995.

Matsuoka, A., E. Boss, M. Babin, L. Karp-Boss, M. Hafez, A. Chekalyuk, C. Poctor, P.J. Werdell, and A. Bricaud. 2017. Pan-Arctic optical characteristics of colored dissolved organic matter: Tracing dissolved organic carbon in changing Arctic waters using satellite ocean color data. *Rem. Sens. Environ.* 200: 89–101.

McDowell, W.H. 1985. Kinetics and mechanisms of dissolved organic carbon retention in a headwater stream. *Biogeochemistry* 1: 329–352.

Medeiros, P.M. 2022. The effects of hurricanes and storms on the composition of dissolved organic matter in a Southeastern U.S. Estuary. *Frontiers in Marine Sciences* 9: 855720.

Medeiros, P.M., M. Seidel, T. Dittmar, W.B. Whitman, and M.A. Moran. 2015. Drought-induced variability in dissolved organic matter composition in a marsh-dominated estuary. *Geophysical Research Letters* 42: 6446–6453. https://doi.org/10.1002/2015GL064653.

Medeiros, P.M., L. Babcock-Adams, M. Seidel, R.M. Castelao, D. Di Iorio, J.T. Hollibaugh, et al. 2017. Export of terrigenous dissolved organic matter in a broad continental shelf. *Limnology and Oceanography* 62: 1718–1731. https://doi.org/10.1002/lno.10528.

Miller, R.L., M.M. Brown, and R.P. Mulligan. 2016. Transport and transformation of dissolved organic matter in the Neuse River estuarine system, NC, USA, following Hurricane Irene (2011). *Marine & Freshwater Research* 67: 1313–1325.

Moran, M.A., W. Sheldon, and J. Sheldon. 1999. Biodegradation of riverine dissolved organic carbon in five estuaries of the southeastern United States. *Estuaries* 22: 55–64.

Moran, M.A., E.B. Kujawinski, A. Stubbins, R. Fatland, L. Aluwihare, A. Buchan, et al. 2016. Deciphering ocean carbon in a changing world. *Proceedings of the National Academy of Sciences* 113: 3143–3151.

Noriega, C., and M. Araujo. 2014. Carbon dioxide emissions from estuaries of northern and northeastern Brazil. *Science and Reports* 4: 6164.

Osburn, C.L., M.P. Mikan, J.R. Etheridge, M.R. Burchell, and F. Birgand. 2015. Seasonal variation in the quality of dissolved and particulate organic matter exchanged between a saltmarsh and its adjacent estuary. *Journal of Geophysical Research. Biogeosciences* 120: 1430–1449. https://doi.org/10.1002/2014JG002897.

Osburn, C.L., J.N. Atar, T.J. Boyd, and M.T. Montgomery. 2019. Antecedent precipitation influences the bacterial processing of terrestrial dissolved organic matter in a North Carolina estuary. *Estuarine, Coastal and Shelf Science* 221: 119–131.

Overland, J., R. Preisendorfer, and R. 1982. A significance test for principal components applied to a cyclone climatology. *Monthly Weather Review* 110 (1): 1–4. https://doi.org/10.1175/1520-0493(1982)110%3c0001:ASTFPC%3e2.0.CO;2.

Paerl, H.W., J.R. Crosswell, B. van Dam, N.S. Hall, K.L. Rossignol, C. Osburn, et al. 2018. Two decades of tropical cyclone impacts on North Carolina's estuarine carbon, nutrient and phytoplankton dynamics: Implications for biogeochemical cycling and water quality in a stormier world. *Biogeochemistry* 141: 307–332.

Raymond, P., and J. Bauer. 2000. Bacterial consumption of DOC during transport through a temperate estuary. *Aquatic Microbial Ecology* 22: 1–12.

Raymond, P.A., J.E. Saiers, and W.V. Sobczak. 2016. Hydrological and biogeochemical controls on watershed dissolved organic matter transport: Pulse-shunt concept. *Ecology* 97: 5–16.

Reichstetter, M., P. Fearns, S. Weeks, L. McKinna, C. Roelfsema, and M. Furnas. 2015. Bottom reflectance in ocean color satellite remote sensing for coral reef environments. *Remote Sens.* 7 (12): 16756–16777.

Rudolph, J.C., C.A. Arendt, A.G. Hounshell, H.W. Paerl, and C.L. Osburn. 2020. Use of geospatial, hydrologic, and geochemical modeling to determine the influence of wetland-derived organic matter in coastal waters in response to extreme weather events. *Frontiers in Marine Science* 7: 18. https://doi.org/10.3389/fmars.2020.00018.

Salisbury, J., D. Vandemark, J. Campbell, C. Hunt, D. Wisser, N. Reul, and B. Chapron. 2011. Spatial and temporal coherence between Amazon River discharge, salinity, and light absorption by colored organic carbon in western tropical Atlantic surface waters. *Journal of Geophysical Research* 116 (C7): C02028.

Santoso, A., M.J. Mcphaden, and W. Cai. 2017. The defining characteristics of ENSO extremes and the strong 2015/2016 El Niño. *Reviews of Geophysics* 55: 1079–1129. https://doi.org/10.1002/2017RG000560.

Schiebel, H.N., G.B. Gardner, X. Wang, F. Peri, and R.F. Chen. 2018. Seasonal export of dissolved organic matter from a New England salt marsh. *Journal of Coastal Research* 34: 939–954.

Seidel, M., T. Dittmar, N.D. Ward, A.V. Krusche, J.E. Richey, P.L. Yager, and P.M. Medeiros. 2016. Seasonal and spatial variability of dissolved organic matter composition in the lower Amazon River. *Biogeochemistry* 131: 281–302.

Sharp, J.H., K. Yoshiyama, A. Parker, M. Schwartz, S. Curless, A. Beauregard, J. Ossolinki, and A. Davis. 2009. A biogeochemical view of estuarine eutrophication: Seasonal and spatial trends and correlations in the Delaware Estuary. *Estuaries and Coasts* 32: 1023–1043.

Singh, S., S. Inamdar, M. Mitchell, and P. McHale. 2014. Seasonal pattern of dissolved organic matter (DOM) in watershed sources: Influence of hydrologic flow paths and autumn leaf fall. *Biogeochemistry* 118: 321–337. https://doi.org/10.1007/s10533-013-9934-1.

Spencer, R.G.M., K.D. Butler, and G.R. Aiken. 2012. Dissolved organic carbon and chromophoric dissolved organic matter properties of rivers in the USA. *Journal of Geophysical Research* 117: G03001. https://doi.org/10.1029/2011JG001928.

Spivak, A., J. Sanderman, J. Bowen, E. Canuel, and C. Hopkinson. 2019. Global-change controls on soil-carbon accumulation and loss in coastal vegetated ecosystems. *Nature Geoscience* 12: 685–692.

Tzortziou, M., P.J. Neale, C.L. Osburn, J.P. Megonigal, N. Maie, and R. Jaffé. 2008. Tidal marshes as a source of optically and chemically distinctive colored dissolved organic matter in the Chesapeake Bay. *Limnology and Oceanography* 53 (1): 148–159.

Wang, Y., R.M. Castelao, and D. Di Iorio. 2017. Salinity variability and water exchange in interconnected estuaries. *Estuaries and Coast* 40: 917–929.

Ward, N.D., J.P. Megonigal, B. Bond-Lamberty, V.L. Bailey, D. Butman, E.A. Canuel, et al. 2020. Representing the function and sensitivity of coastal interfaces in Earth system models. *Nature Communications* 11 (1): 1–14.

Yamaguchi, H., J. Ishizaka, E. Siswanto, Y. Baek Son, S. Yoo, and Y. Kiyomoto. 2013. Seasonal and spring interannual variations in satellite-observed chlorophyll-a in the Yellow and East China

Seas: New datasets with reduced interference from high concentration of resuspended sediment. *Continental Shelf Research* 59: 1–9.

Yoon, B., and P.A. Raymond. 2012. Dissolved organic matter export from a forested watershed during Hurricane Irene. *Geophysical Research Letters* 39: 1–6.

Chen, C., G. Cowles, and R.C. Beardsley. 2006a. An unstructured grid, finite-volume coastal ocean model: FVCOM user manual, 2nd ed., SMAST/UMASSD Tech. Rep. 06–0602, 315. New Bedford, MA: School for Marine Science and Technology, University of Massachusetts-Dartmouth.

Letourneau, M. L., S. C. Schaefer, H, Chen, A. M. McKenna, M. Alber, and P. M. Medeiros. 2021. Spatio-temporal changes in dissolved organic matter composition along the salinity gradient of a marsh-influenced estuarine complex. *Limnol. Oceanogr.* 66, 3040–3054

Mooers, C. N., L. Bogert, R. Smith and J. Pattullo. 1968. A compilation of observations from moored current meters and thermographs. Data Rep. 30 Dept. Oceanogr. Oregon State University, Corvallis, 91–92.

Odum, E.P. 1980. The status of three ecosystem-level hypotheses regarding salt marsh estuaries: tidal subsidy, outwelling, and detritus-based food chains. In Estuarine perspectives (pp. 485–495). Academic Press.

Tebeau, P.A., and T.N. Lee. 1979. Wind induced circulation on the Georgia shelf, (winter 1976/77) RSMAS Tech Rep. 79003. Miami, Fla: Univ. of Miami.

Wolfe, D. and B. Kjerfve. 1986. Estuarine variability: an overview. In Estuarine Variability, 3–17.